

# A Site-Specific Stochastic Propagation Model for Passive UHF RFID

Antonios G. Dimitriou, *Senior Member, IEEE*, Stavroula Siachalou, Aggelos Bletsas, *Senior Member, IEEE*  
and John N. Sahalos, *Life Fellow, IEEE*

**Abstract**—This letter proposes a computationally inexpensive, site-specific propagation model, useful in coverage evaluation of RFID networks with passive tags. The parameters of a Rice distribution for each point in the volume of interest are computed using site-specific approximations that address overall space geometry, materials and polarization. The probability of successful identification of passive RFID tags is calculated. Coverage statistics and performance evaluation of complex RFID networks can be quickly conducted. Experimental results at the UHF regime corroborate the accuracy of the model.

**Index Terms**—Radiofrequency identification, UHF propagation, Ray tracing, Stochastic processes, Rician channels.

## I. INTRODUCTION

RADIO Frequency Identification (RFID) is considered a key enabler for the "Internet of Things", as well as the logistics industry [1]. The planning problem of RFID network involves the selection of appropriate antenna locations so that a given cost function, e.g. number of antennas, is minimized under specific quality constraints, e.g. identification percentage in the target volume [2], [3]. Due to the small range of RFID systems involving passive tags, propagation data from thousands of candidate antenna-configurations must be extracted, in order to decide on the topology of a large area network. The running time of existing computational electromagnetic methods [4] or analytical ray-tracing [5] is prohibitive for such estimations.

Typically, for such computationally-demanding problems, simple propagation models are considered, such as the Friis free-space formula or empirical models. A representative example is the two-slope model [6], on top of which stochastic fading might be considered [7], where slope and the break-point distance is derived from measurements. However, coverage estimation from non site-specific models ignore important parameters of the propagation space (e.g. geometry and materials). An interesting, computationally inexpensive alternative was proposed in [8]: the minimum reception level of the interference pattern created from the phase-sum of the

direct field and the singly reflected field from the wall opposite to the antenna defines an ellipsoid as the "useful reading region". Though the model in [8] can be applied for single antenna configurations, it cannot quantify the identification performance of multiple reader-antennas with overlapping coverage-regions, operating in the same area.

In this paper, we calculate the probability of successful identification of passive RFID tags, assuming Rician fading [9]. Rician fading is valid when a strong component dominates the reception pattern. Due to the power constraints of battery-less RFID technology, the multi-path reception pattern is expected to include a strong Line Of Sight (LOS) path. Specular components, namely LOS and multiple reflections, dominate the total received field for such short-range LOS conditions with respect to multipath originating from other scatterers [10], [11]. In contrast to prior art, where a specific Rice probability density function (pdf) is considered in the entire room, we derive different pdfs for each calculation point inside the volume of interest, because we expect different relationships between the power of the direct contribution with respect to the power carried by all other components; these parameters are locally affected by the radiation pattern of the antennas and the geometrical relationships with the surrounding environment, mapped in the reflection coefficients.  $K$ -ratio of the Rice pdf demonstrates 20dB variability in the same room.

Specifically, this paper offers a computationally inexpensive model and method to separately calculate the proper pdf for each point in the entire volume of interest. For each wall, we consider a ray cluster that includes all multiply reflected components that initially bounce on the same wall. We discard the phase term of each ray in the cluster and evaluate the average power of the entire cluster. As a consequence, we do not predict the exact locations of maxima and minima of the field for a given frequency, as in classical ray-tracing models, but we calculate the probability that such an event may take place for each location. To accomplish that in reduced time for each tag's position, we calculate exactly the power of the direct path and only of the singly reflected ray for each cluster. The power of the cluster, including the higher order terms, is then approximated by a simple expression derived herein. The proposed model carefully considers radiation pattern, geometry and materials of the surrounding walls, as well as polarization of both reader and tag antenna; the latter is crucial for RFID applications [5], [12]. The model is presented for the reader-to-tag link, because passive UHF RFID systems are typically forward link limited [12]. However, it can be directly extended to the round-trip link, for monostatic or bistatic

This work was supported by the ERC-04-BLASE project, executed in the context of the Education & Lifelong Learning Program of General Secretariat for Research & Technology (GSRT) and funded through European Union-European Social Fund and national funds. A. G. Dimitriou and S. Siachalou are with School of Electrical and Computer Engineering, Aristotle University of Thessaloniki, 54636, Thessaloniki, Greece ([antodimi,ssiachal@auth.gr](mailto:antodimi,ssiachal@auth.gr)). A. Bletsas is with School of Electronics and Computer Engineering, Technical University of Crete, Kounoupidiana Campus, 73100 Chania Crete, Greece ([aggelos@telecom.tuc.gr](mailto:aggelos@telecom.tuc.gr)). J. N. Sahalos is with University of Nicosia, Dept. of Electrical and Computer Engineering, 46 Makedonitissas Avenue 24005 Nicosia, Cyprus ([sahalos.j@unic.ac.cy](mailto:sahalos.j@unic.ac.cy)).

configurations. Comparison with ray tracing and experimental results corroborate the accuracy of the proposed model.

## II. DERIVATION OF THE MODEL

### A. Stochastic Model - Rice Distribution

The Rice pdf is given by:

$$f(x|\nu, \sigma) = \frac{x}{\sigma^2} e^{\left(\frac{-(x^2 + \nu^2)}{2\sigma^2}\right)} I_0\left(\frac{x\nu}{\sigma^2}\right), \quad (1)$$

where  $\nu^2$  is the power of the LOS path,  $2\sigma^2$  is the average power of the other contributions  $x$  is the signal's amplitude and  $I_0(z)$  is the modified Bessel function of the first kind and zero order. The cumulative distribution function (cdf) is given by:

$$F_x(x|\nu, \sigma) = 1 - Q_1\left(\frac{\nu}{\sigma}, \frac{x}{\sigma}\right), \quad (2)$$

where  $Q_1(a, b)$  is the Marcum Q-function. Parameters  $\nu^2$  and  $2\sigma^2$  are separately calculated in each position in the volume of interest. Though  $\nu^2$  is directly calculated by a closed form expression of the LOS contribution,  $2\sigma^2$  involves more complex, time-demanding calculations of the multi-path contributions. A fast prototype method is presented next to evaluate the above Rice pdf parameters from the contributions of the multiply reflected rays among opposite walls. Diffraction from corners is not considered, because it is expected to have minor contribution on the total scattered power, while scattering from smaller, often non-mapped, objects is expected to have a small and local influence on fading.

### B. Multiple Reflections

Consider a transmitting antenna and a tag inside a room, as shown in Fig. 1. Let  $\mathbf{E}_{\text{inc}}(r, \phi, \theta)$  represent the incident field's vector that has traveled a path of length  $r$  at the direction defined by horizontal and vertical angles  $\phi, \theta$  respectively. The magnitude of  $\mathbf{E}_{\text{inc}}(r, \phi, \theta)$  is:

$$|\mathbf{E}_{\text{inc}}(r, \phi, \theta)| = \sqrt{\frac{\eta W_t G_t(\phi, \theta)}{2\pi}} \frac{1}{r}. \quad (3)$$

$W_t$  is the power of the transmitted carrier,  $G_t(\phi, \theta)$  is the transmitting antenna's gain and  $\eta$  is the free-space impedance.

Consider that a ray, transmitted at the direction defined by angles  $\phi_1, \theta_1$ , is reflected once on the vertical wall to the right of the antenna and travels a path of length  $r_1$  until it reaches the tag. The singly reflected field at the tag can be written as the sum of two vectors:

$$\begin{aligned} \mathbf{E}_{\mathbf{r}}(r_1, \phi_1, \theta_1) &= \mathbf{E}_{\mathbf{r}}^{\perp}(r_1, \phi_1, \theta_1) + \mathbf{E}_{\mathbf{r}}^{\parallel}(r_1, \phi_1, \theta_1) = \\ &|\mathbf{E}_{\text{inc}}(r_1, \phi_1, \theta_1)| \cos(\psi) |\Gamma_1^{\perp}| e^{i(\omega t + \beta_{\text{inc}}^{\perp} + \beta_{\Gamma_1}^{\perp} + kr_1)} \hat{\eta}_0 + \\ &|\mathbf{E}_{\text{inc}}(r_1, \phi_1, \theta_1)| \sin(\psi) |\Gamma_1^{\parallel}| e^{i(\omega t + \beta_{\text{inc}}^{\parallel} + \beta_{\Gamma_1}^{\parallel} + kr_1)} \hat{\epsilon}_0, \quad (4) \end{aligned}$$

where  $\mathbf{E}_{\mathbf{r}}^{\perp}(r_1, \phi_1, \theta_1)$ ,  $\mathbf{E}_{\mathbf{r}}^{\parallel}(r_1, \phi_1, \theta_1)$  represent the field's vectors perpendicular and parallel to the plane of incidence at the directions defined by unit vectors  $\hat{\eta}_0, \hat{\epsilon}_0$  respectively,  $\omega = 2\pi f$ ,  $f$  is the considered frequency,  $\beta_{\text{inc}}^{\perp}$  and  $\beta_{\text{inc}}^{\parallel}$  are the phases of the perpendicular and vertical components of

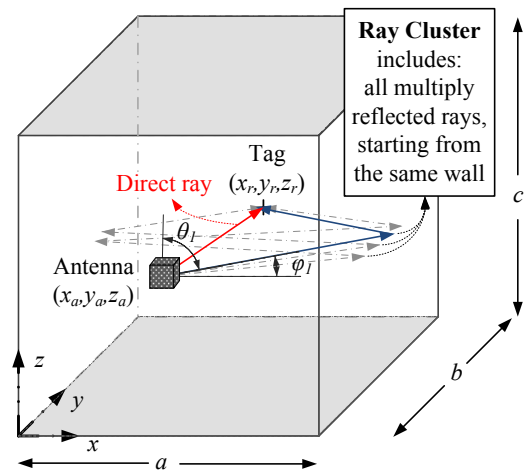


Fig. 1. Representation of a typical room.

the incident field's vectors, so that elliptical polarization can be modeled,  $k = 2\pi/\lambda$  and  $\lambda$  is the considered wavelength. In (4),  $\psi$  is the angle of the incident field vector with the unit vector  $\hat{\eta}_0$ , perpendicular to the plane of incidence and  $|\mathbf{E}_{\text{inc}}(r_1, \phi_1, \theta_1)|$  is given by substituting in (3). The reflection coefficients  $\Gamma_1^{\perp}$  and  $\Gamma_1^{\parallel}$  are both complex with phases  $\beta_{\Gamma_1}^{\perp}$  and  $\beta_{\Gamma_1}^{\parallel}$  respectively.

Consider a ray that is multiply reflected  $n$ -times among opposite parallel walls. The field expression of the  $n$ -times reflected ray includes the 1<sup>st</sup> order reflection coefficient raised in the power of  $n$  and the phase term changed accordingly:

$$\begin{aligned} \mathbf{E}_{\mathbf{r}}(r_n, \phi_n, \theta_n) &= \mathbf{E}_{\mathbf{r}}^{\perp}(r_n, \phi_n, \theta_n) + \mathbf{E}_{\mathbf{r}}^{\parallel}(r_n, \phi_n, \theta_n) = \\ &|\mathbf{E}_{\text{inc}}(r_n, \phi_n, \theta_n)| \cos(\psi_n) |\Gamma_n^{\perp}|^n e^{i(\omega t + \beta_{\text{inc}_n}^{\perp} + n\beta_{\Gamma_n}^{\perp} + kr_n)} \hat{\eta}_{0n} + \\ &|\mathbf{E}_{\text{inc}}(r_n, \phi_n, \theta_n)| \sin(\psi_n) |\Gamma_n^{\parallel}|^n e^{i(\omega t + \beta_{\text{inc}_n}^{\parallel} + n\beta_{\Gamma_n}^{\parallel} + kr_n)} \hat{\epsilon}_{0n}. \quad (5) \end{aligned}$$

In (5), all variables that are different with respect to their value in (4) are substituted with the subscript  $n$ . We observe that each higher order reflection term is expected to contribute less in the total power as it has traveled a longer path and the reflection coefficient is raised in a greater power. In order to accelerate the calculations and reduce the complexity of the proposed model, we approximate the angles of departures of higher order terms of each ray-cluster to that of the singly reflected ray of the cluster:

$$(\phi_n, \theta_n) = (\phi_1, \theta_1), \psi_n = \psi, \hat{\eta}_{0n} = \hat{\eta}_0, \hat{\epsilon}_{0n} = \hat{\epsilon}_0. \quad (6)$$

Due to the above geometrical approximations, we have:

$$\begin{aligned} \Gamma_n^{\perp} &= \Gamma_1^{\perp}, \beta_{\Gamma_n}^{\perp} = \beta_{\Gamma_1}^{\perp}, \beta_{\text{inc}_n}^{\perp} = \beta_{\text{inc}}^{\perp}, \Gamma_n^{\parallel} = \Gamma_1^{\parallel}, \\ \beta_{\Gamma_n}^{\parallel} &= \beta_{\Gamma_1}^{\parallel}, \beta_{\text{inc}_n}^{\parallel} = \beta_{\text{inc}}^{\parallel}. \quad (7) \end{aligned}$$

The errors, due to this approximation were found to be small, as will be shown in the results, because the strongest component of each ray cluster is exactly calculated. If higher accuracy is sought, one may calculate exactly additional higher order reflection terms at the expense of increased complexity

and running-time. The multiply reflected field for each ray-cluster is given by the following vector sum:

$$\mathbf{E}_{\text{reff}} = \sqrt{\frac{\eta W_t G_t(\phi_1, \theta_1)}{2\pi}} \left( \cos(\psi) \sum_n \frac{|G_I^\perp|^n e^{i(\omega t + \beta_{inc}^\perp + n\beta_r^\perp + kr_n)}}{r_n} \hat{\eta}_0 + \sin(\psi) \sum_n \frac{|G_I^\parallel|^n e^{i(\omega t + \beta_{inc}^\parallel + n\beta_r^\parallel + kr_n)}}{r_n} \hat{\epsilon}_0 \right) \quad (8)$$

In a static environment and for a specific frequency, the field inside the propagation area should be constant (with specific maxima and minima). However, from a propagation-estimation perspective, prediction of the exact field may not be possible. The phase information of the rays in (8) is sensitive to the following typical errors: inaccurate modeling of the electromagnetic properties of the surrounding walls, room-dimensions or antenna-placement/tilting imprecisions, moving people. Any such inaccuracy will result in a significant phase error, thus changing the field of equation (8). Also notice that the phases of different rays in (8) are not correlated, because they travel path lengths with differences in the order of several wavelengths. In order to calculate the average power of each ray-cluster, given the uncertainty of the phase of each contribution, we consider the phases of the rays as random variables, identically and independently distributed, uniformly over  $[0, 2\pi]$ . A different way to validate this assumption is to view each calculation-point as the center of a small sphere with diameter in the order of a wavelength so that minima and maxima of the field occur in different locations of the sphere, where nearly similar (in magnitude) components add with different phases. In order to calculate the average power (over phase) of the field in the sphere, we can consider the sum of vectors with known magnitudes and random phases uniformly distributed over  $[0, 2\pi]$ , given by [13]:

$$P_{\hat{\eta}_0} = A \cos^2(\psi) \sum_n \frac{(|G_I^\perp|^2)^n}{r_n^2},$$

$$P_{\hat{\epsilon}_0} = A \sin^2(\psi) \sum_n \frac{(|G_I^\parallel|^2)^n}{r_n^2}, \quad A = \frac{\lambda^2 W_t G_t(\phi_1, \theta_1)}{(4\pi)^2}. \quad (9)$$

$P_{\hat{\eta}_0}$ ,  $P_{\hat{\epsilon}_0}$  represent the power along a receiving antenna with unity gain on the two polarization axes  $\hat{\eta}_0$ ,  $\hat{\epsilon}_0$ , respectively.

Let  $(x_a, y_a, z_a)$ ,  $(x_r, y_r, z_r)$  represent the coordinates of the transmitting and receiving antennas, respectively and  $(a, b, c)$  represent the room's dimensions, as shown in Fig. 1. Evaluating  $r_n$  for the multiple reflections taking place among the two vertical walls, we have:

$$r_n^2 = (y_a - y_r)^2 + (z_a - z_r)^2 + \Delta x_n^2. \quad (10)$$

$\Delta x_n$  is the projection of the total traveled path of the n-times reflected ray on the  $x$ -axis of the coordinate system of Fig. 1. It can be shown that the average increase of the length of  $\Delta x_n$  for each additional reflection is  $a$  (for each additional reflection, the ray will traverse the room one more time). In an effort to simplify the expression and reduce the computational complexity, we approximate  $\Delta x_n$  by  $\Delta x_n = \Delta x_1 + (n-1)a$ .

Similarly, for multiple reflections taking place along the  $y$  and  $z$  axes, we have  $\Delta y_n = \Delta y_1 + (n-1)b$  and  $\Delta z_n = \Delta z_1 + (n-1)c$ , respectively. By substituting in (9), we have:

$$P_{\hat{\eta}_0} = A \cos^2(\psi) \sum_{n=1}^N \frac{(|G_I^\perp|^2)^n}{(y_a - y_r)^2 + (z_a - z_r)^2 + \Delta x_n^2},$$

$$P_{\hat{\epsilon}_0} = A \sin^2(\psi) \sum_{n=1}^N \frac{(|G_I^\parallel|^2)^n}{(y_a - y_r)^2 + (z_a - z_r)^2 + \Delta x_n^2},$$

where  $\Delta x_n = \Delta x_1 + (n-1)a$ . (11)

$N$  is the number of reflections considered from each wall. Eq. (11) represents a closed-form approximation of the average power of the cluster of reflected rays originating from the wall to the right of the antenna. In order to apply (11), one should calculate explicitly only the 1<sup>st</sup> order reflection term from the specific wall. The power along any polarization axis is calculated, by projecting the estimations to the desired axis. To finish the model and calculate the total power of the multiply reflected rays at each location of interest, we must re-apply (11) for the remaining 5 walls in the room and sum all power-contributions on the polarization axes of interest.

### C. Application of the Proposed Model

We consider a calculations' grid with  $M$  points in the volume of interest. A tag is considered successfully identified if the voltage at the tag's IC is greater than its "wake-up" threshold  $\gamma$ . The identification-probability at grid-point  $l$  is:

$$P_l(X \geq \gamma) = 1 - F_x(\gamma|\nu_l, \sigma_l). \quad (12)$$

$F_x(\gamma|\nu_l, \sigma_l)$  is given in (2);  $\nu_l^2$  is the power of the LOS path, the field expression is given in (3), on the polarization axis of the tag and  $2\sigma_l^2$  is the power of the multiply reflected rays, calculated by applying (11) for the surrounding walls. Let  $U(\gamma)$  represent the percentage of the volume of interest  $V$ , where successful identification of passive tags is accomplished [13] (ch. 4):

$$U(\gamma) = \frac{1}{V} \int_V P_{dV}(X \geq \gamma) dV = \frac{1}{V} \sum_{l=1}^M P_l(X \geq \gamma) dV_l \quad (13)$$

For a cubic calculations' grid, with equal spacing among grid points, (13) reduces to  $U(\gamma) = \sum_{l=1}^M P_l(X \geq \gamma)/M$ .

1) *Comparison with analytical calculations and measurements:* In Fig. 2, the results from comparing the proposed model with analytical ray-tracing and measurements conducted in a  $3.5m \times 3m$  room are presented. Equations (12)-(13) are employed for the calculation of the identification percentage per polarization axis and (11) for the estimation of the average scattered power at the calculations' grid. For the measurements, 200 orthogonally polarized passive UHF RFID tags were fixed on threads, forming a cubic measurements' grid, shown in Fig. 2. By reducing the transmitted power from a 7dBic circularly polarized antenna at 1dB-step, we counted the number of successfully identified passive RFID tags per polarization axis. For the analytical ray-tracing model, the phase sum of all contributions is estimated at the same

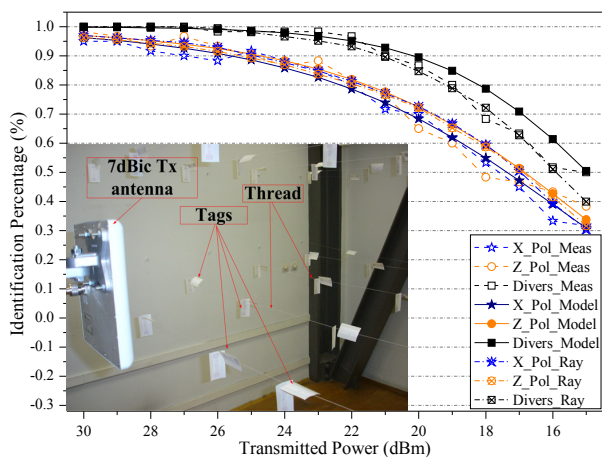


Fig. 2. Comparison between predictions and measurements.

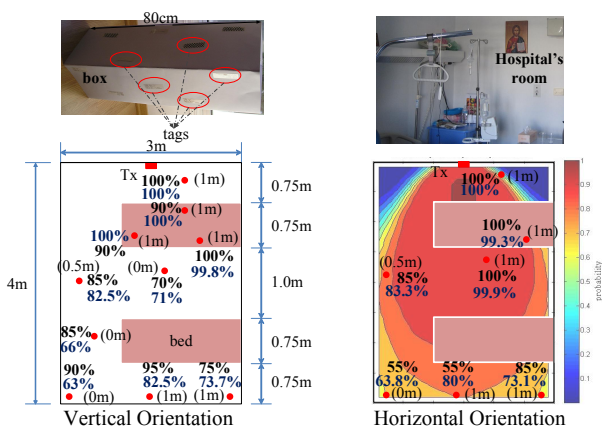


Fig. 3. Comparison with measurements in hospital room.

calculations' grid. Good agreement is recorded for both polarizations and for polarization-diversity between the proposed model and the measurements or the ray-tracing estimations (mean absolute error from 0.01 to 0.035). Details on the measurements' procedure can be found in [5]. The model was compared with measurements from additional configurations, demonstrated in [5], where good agreement was recorded as well.

Comparison with measurements in a hospital's room, including several non-modeled scatterers, are presented in Fig. 3. A box with 20 tags is moved around the room and for each location, we compare the number of identified tags with the corresponding estimation. Next to each sample are shown: the distance of the box from the ground (in parenthesis), the measured (black) and the estimated (blue) percentage. An estimation probability-result (shown faded), is demonstrated in the horizontal polarization subfigure for tag-height  $z=1m$ . Good agreement is recorded in 14 out of 17 locations. The error in some locations may be due to the limited number of samples (20) per location and the local effects of non-mapped objects. The mean absolute error was 0.083 for the vertical polarization and 0.048 for the horizontal.

Two characteristic results are demonstrated in Fig. 4. The 1<sup>st</sup>, showing the probability of successful identification for

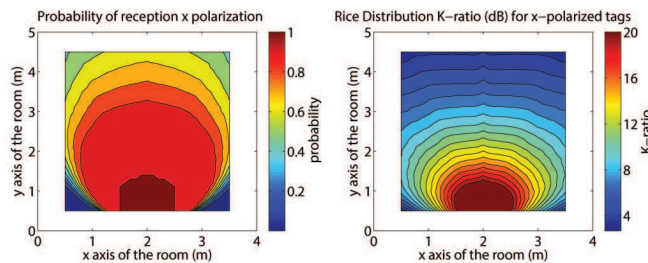


Fig. 4. Probability of reception for x-polarized tags at  $z=1.3m$  for  $\gamma$ , corresponding to  $-14dBm$  and  $K$ -ratio of the corresponding pdfs.

x-polarized tags at  $z=1.1m$  above the ground, gives visual inspection of the performance of the examined antenna-configuration. The 2<sup>nd</sup>, showing the variation of the  $K$ -ratio in dB,  $K = 10 \log_{10}(\nu^2/2\sigma^2)$ , of the "Rice" pdf in the area, verifies the variability of fading in the area of interest. Notice that  $K$  experiences a large 20dBs variation with the largest  $K$ -values taking place in the vicinity of the reader's antenna.

### III. DISCUSSION

This work put forth a computationally efficient, site-specific, stochastic model to evaluate the identification performance of passive RFID systems. Finally, it should be emphasized that, since the pdf of the power-reception profile is extracted at each location, the performance of different multipath-compensation techniques, e.g. polarization diversity, interaction of multi-antenna systems [5] (in an RFID network), can be analytically calculated in any environment.

### REFERENCES

- [1] D. M. Dobkin, *The RF in RFID: Passive UHF RFID in Practice*, Oxford, Boston, Newnes (Elsevier), 2007.
- [2] A. Bahri, S. Chamberland, "On the wireless local area network design problem with performance guarantees", *Elsevier Computer Networks*, vol. 48, no. 6, pp. 856-866, Aug. 2005.
- [3] E. Di Giampaolo, F. Forni, and G. Marrocco, "RFID-network planning by Particle Swarm Optimization," in *Proc. EuCAP*, 2010.
- [4] C. A. Balanis, *Advanced Engineering Electromagnetics, 2nd Ed.*, New Jersey, John Wiley & Sons, 2012.
- [5] A. G. Dimitriou, A. Bletsas, and J. N. Sahalos, "Room coverage improvements of UHF RFID with commodity hardware," *IEEE Antennas Propag. Mag.*, vol. 53, pp. 175-194, Feb. 2011.
- [6] M. F. Iskander and Z. Yun, "Propagation prediction models for wireless communication systems," *IEEE Trans. Microw. Theory Techn.*, vol. MTT-50, pp. 662-673, March 2002.
- [7] A. Lazaro., D. Girbau, and D. Salinas, "Radio link budgets for UHF RFID on multipath environments", *IEEE Trans. Antennas Propag.*, vol. AP-57, pp. 1241-1251, April 2009.
- [8] G. Marrocco, E. Di Giampaolo, and R. Aliberti., "Estimation of UHF RFID reading regions in real environments", *IEEE Antennas Propag. Mag.*, vol. 51, pp. 44-57, Dec. 2009.
- [9] S. O. Rice, "Mathematical analysis of random noise", *Bell System Technical Journal*, vol. 24, pp. 46156, 1945.
- [10] J. Poutanen, J. Salmi, K. Haneda, V.-M. Kolmonen, and P. Vainikainen, "Angular and shadowing characteristics of dense multipath components in indoor radio channels," *IEEE Trans. Antennas Propag.*, vol. AP-59, pp. 1-9, Jan. 2011.
- [11] D. Kim, M. A. Ingram, and W. W. Smith Jr., "Measurements of small-scale fading and path loss for long range RF tags," *IEEE Trans. Antennas Propag.*, vol. AP-51, pp. 17401749, Aug. 2003.
- [12] J. D. Griffin, and G. D. Durgin, "Complete link budgets for backscatter-radio and RFID systems", *IEEE Antennas Propag. Mag.*, vol. 51, pp. 11-25, April 2009.
- [13] T. S. Rappaport, "Mobile Radio Propagation: Small Scale Fading and Multipath" in *Wireless Communications Principles and Practice*, 2nd Ed. Prentice Hall, 2001.